International Journal of Current Advanced Research
ISSN: O: 2319-6475, ISSN: P: 2319-6505, Impact Factor: SJIF: 5.995
Available Online at www.journalijcar.org
Volume 7; Issue 1(H); January 2018; Page No. 9283-9288
DOI: http://dx.doi.org/10.24327/ijcar.2018.9288.1529

Research Article

PREPARATION OF MoS_2–GRAPHENE COMPOSITES WITH EXCELLENT PHOTOCATALYTIC ACTIVITY UNDER VISIBLE LIGHT

Komal M Sarode, Umesh D Patil and Dilip R Patil*

Nanomaterial Research Laboratory, R.C. Patel ACS College, Shirpur, 425405, Maharashtra, India

A R T I C L E I N F O

Article History:

Received 14th October, 2017
Received in revised form 10th November, 2017
Accepted 26th December, 2017
Published online 28th January, 2018

Key words:

Graphene oxide; MoS2/RGO composites; pollutant; photocatalysis.

A B S T R A C T

In this work, MoS_2-graphenecomposites (MoS2/RGO) were successfully synthesized via hydrolysis of lithiated MoS_2 ($LiMoS_2$). The obtained products as well as the photocatalytic activities in the degradation of Rhodamine B(RhB) were characterized by X-ray diffraction, Field Emission scanning electron microscopy, High resolution transmission electron microscopy, Fourier transform infrared spectroscopy, Raman spectroscopy and UV-Vis absorption spectroscopy, respectively. The result shown that MoS_2/RGO composite exhibit excellent photocatalytic performance than to Restack MoS_2, with nearly 90% of RhB degraded after visible light irradiation for 30 min. This excellent photocatalytic activity could be attributed to the synergistic effect that arises between the MoS_2 and RGO, which significantly reduces electron–hole pair recombination. Moreover, the possible photocatalytic mechanism of MoS_2/RGO composites was also proposed.

INTRODUCTION

Nowadays, Photocatalytic degradation technique is an important approach to address environmental pollution. Commonly, organic dyes used from leathers, textile, fabric, food, cosmetics and paper industries have caused critical environmental problems, as some of the dye wastewater from these industries can pollute ground water resources, and their utilization has many toxic and harmful effects on human beings. Semiconducting based photocatalysts have ability to solve the serious environmental pollution because of their superior physical and chemical property [1-4]. Searching for visible light responsive photocatalyst has attracted much attention of the researchers.

Molybdenum disulfide (MoS_2) is a semiconductor material with a narrow band gap (~1.8 eV) exhibits very high light absorption in visible spectrumregion [5, 6], which is quite beneficial to photocatalytic applications [7-10]. However, quick recombination of photogenerated charge carriers and low conductivity coefficients significantly limits the practical applications of MoS_2[11]. Based on previously data reported in literature, if it is coupled with conductive material could help the separation of photogenerated electron–hole recombination, thus improving the photocatalytic performance(12, 13). Graphene, a versatile carbon material with a single layer and a sp^2-hybridized carbon atom, exhibits high surface area,excellent electrical and thermal properties [14-17]. As graphene can serve as an excellent charge carrier for semiconductors at room temperature[18, 19]. Due to these properties, graphene as an excellent electron-accept or/transport materialhas been applied to improve photocatalysis performancebecause it can separate the photo-generated electron-hole recombination and improve the light adsorption [20-24]. Moreover, it shows enhanced absorption in visible region due to exceptional optical, electronic properties and enhanced pollutant adsorption on photocatalyst is an additional advantage of grapheme [14,25-26]. In this work, we used a by hydrolysis of lithiated MoS_2 ($LiMoS_2$) method to prepare MoS_2/RGO composites, and their photocatalytic performances in the degradation of RhB under visible light irradiation were investigated. The HRTEM images demonstrated that MoS_2 nanosheets were well stack on the graphene sheets (RGO). The MoS_2/RGO composites exhibited high photocatalytic performance in the degradation of RhB under visible light irradiation compared with the Restacked MoS_2.

Corresponding author:* **Dilip R Patil
Nanomaterial Research Laboratory, R.C. Patel ACS College, Shirpur, 425405, Maharashtra, India

Experimental

Synthesis of Graphene oxide (GO)

Graphene oxide was synthesized by the chemical oxidation of graphite flakes by an improved Hummer's method [27]. Typically, 1.5g of graphite flakes was added into a 180 ml: 20 ml mixture of H_2SO_4/H_3PO_4. Subsequently, 9.0g of $KMnO_4$ was added slowly to keep the temperature of the suspension lower than 30°C. Next, the resulting mixture was stirred at

50°C for 12 h. Then, the reaction was cooled down to room temperature and poured onto a mixture of 200 ml of ice and 5ml of 30% H_2O_2. The resultant slurry was washed and centrifuged with 200ml water, 100 ml of 15% HCl, and 100 ml ethanol sequentially. Finally, the remaining solid materials were dried under vacuum for 24 hours.

Synthesis of graphene (RGO)

GO was reduced by hydrazine hydrate in the presence of aqueous medium [28]. Briefly, 500 mg of GO was loaded in 500 ml water and dispersed in an ultrasonic bath cleaner until it became clearwith no visible particulate matter. Afterwards, Hydrazine hydrate (5 ml) was added to the solution and heated in oil bath at 100°C under water cooled condenser for 24 h. Finally, RGO precipitated out as a black solid was isolated by filtration over a medium fritted glass funnel, washed with water and methanol alternately and dried at 50°C in vacuum.

Synthesis of MoS_2/RGOcomposites

In a typical experiment, 1.0g bulk MoS_2 powder was dispersed in the 10 mLof 1.6Mn-butyllithium solution in hexane in a flask filled with N_2gas [29]. The mixture was soaked at room temperature for 48 h. Next, the produced $LixMoS_2$ was filtered and washed repeatedly with hexane to remove excessive lithium and then the dried under the nitrogen atmosphere. Afterward, 100 mg of $LixMoS_2$ was added into 20 ml deionized water and ultrasonicated for 1h to obtained aqueous suspension of MoS_2 nanosheets. The reactions are described as follows: [30]

$$MoS_2 + \text{n-BuLiLi} \longrightarrow MoS_2 + 1/2C_8H_{18} \quad (1)$$

$$LiMoS_2 + H_2O \longrightarrow (MoS_2)_{\text{exfoliated layers}} + LiOH + 1/2H_2 \quad (2)$$

Subsequently, the synthesized RGO nanosheets were dispersed in ethanol (3 mg/mL) and ultrasonicated for 30 min to produce RGO suspension. The produced RGO suspension was then slowly added to the MoS_2 layers and sonicated for 2 h at 10°C. The resultant composite suspension was stirred at room temperature for 3 days and heated in oil bath at 80°C under a water cooled condenser for 24 h. The resultant precipitate was collected by centrifugation at 8000 rpm for 15 min, washed several times with deionized water, ethanol and finally dried in vacuum oven at 80°C overnight. The different mass ratios of $LiMoS_2$/RGO are taken as 100/12.5, 100/25, namedas MG-12 and MG-25.As a control, the restacked MoS_2 was also prepared without adding any RGO.

Photocatalytic experiments

The photocatalytic performances of the prepared samples were evaluated through the photocatalytic degradation of RhB under visible light irradiation. The prepared samples (27 mg) were dispersed into 50ml RhBaqueous solutions (12mg L^{-1}). The suspensions were magnetically stirred in the dark for 30 min to reach the adsorption–desorption equilibrium. The suspensions were exposed to visible light irradiation produced by a 15W white LED light lamp with the main wave create at 450 and 558nm and a color temperature of 6050K. At certain time intervals (5 min), 3 ml of the suspensions were extracted and filtered to remove the photocatalyst. The concentrations of RhB were analyzed by using UV-VIS spectrophotometer.

Characterization

The structure and morphology of the prepared samples were characterized by X-ray diffraction (XRD, EMPYREAN) with Cu-Kα radiation (V = 45 kV, I = 40 mA,λ = 1.54060Å) and field-emission scanning electron microscopy (FESEM, Zeiss/ Ultra 55). The surface morphology of the sample was analyzed using a high-resolution transmission electron microscopy (HRTEM, TecnaiG2, F30). Fourier transform infrared spectroscopy (FT-IR, shimadzu) and Raman spectra (excitation wavelength of 514.5 nm) were also adopted to characterize the prepared samples.

RESULTS AND DISCUSSION

Characterizations of MoS_2/RGO composites

Figure 1 shows the XRD patterns of RGO, bulk MoS_2, restacked MoS_2, and MoS_2/RGO composites. The pure RGO nanosheets exhibit a (002) diffraction peak at 24^0, denoting that the prepared RGO should be an amorphous carbon structure. The bulk MoS_2 of all the sharp diffraction peaks can be ascribed to a hexagonal phase (JCPDS no. 37-1492). The strong peak at 2θ ≅ 14.5 with a d-spacing of 0.64 nm signifies a well-stacked layered structure along the c axis[31]. After lithiation exfoliation, restacked MoS_2 shows broadened (002) peaks and much shortened peak. This Indicates that the mean crystallite size and the number of layers along the c axis are lot of decreases than those of bulk MoS_2 [30, 32]. By comparison, the XRD pattern of MG-12 and MG-25 essentially retains the position of the diffraction peaks of MoS_2, while the intensity of peak continuously decreases. We can also hardly detect the (002) diffraction peak of graphene at 2θ ≅ 24, indicating that the RGO nanosheets seldom stack together.

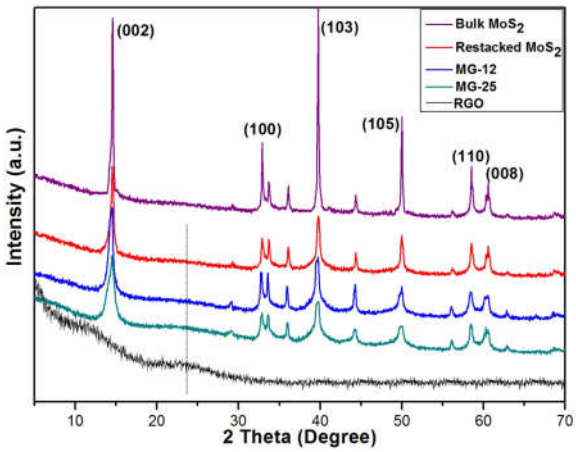

Figure 1.XRD patterns of bulk MoS_2, restacked MoS_2, MG-12, MG-25 and RGO samples.

Fig. 2(a) and (b) show the FESEM images of bulk $MoS_2$and restacked MoS_2. It can be clearly observed that the bulk MoS_2 is largely micrometer-sized inerratic nanosheets, which are tightly stacked together. After lithiation-exfoliation process, the morphology of restacked MoS_2 interestingly changed to highly scattered Nanoflakes. It is also observed that the size and thickness of the nanosheets were significantly decreased relative to the bulk MoS_2. Fig.2(c) shows the FESEM image of RGO material consists of randomly aggregated, thin, crumpled sheets closely associated with each other. As shown in Fig.2(d), the MG-25 exhibits a nanosheet-like morphology, which was formed during the hydrolysis of lithiated MoS_2 ($LiMoS_2$) process. The existence of MoS_2 and RGO in the

composites has been proved by the peaks of C, Mo, S and a small number of O in the EDS spectrum (Fig.2 (e)) also confirm the ratio of Mo and S atoms is 1 to 1.89, which is close to the proportion of MoS_2. Fig. 2(f) shows the HRTEM images of the MG-25, it can be observed that the several layers MoS_2, which are supported on the surface of RGO, the interlayer distance of MoS_2 in MG-25 is 0.61 nm, which is less than that of bulk MoS_2 with an interlayer distance of 0.64 nm. Fourier transforms infrared (FT-IR) spectra of the as-prepared GO, RGO and MG-25 samples are show in Figure 3. The characteristic peaks of GO appear at around 3415 cm^{-1}(O-H stretching vibration), 1735cm^{-1}(C=O stretching vibration), 1620cm^{-1}(C=C stretching vibration), 1390cm^{-1}(C-OH stretching vibration) and 1100 cm^{-}(C-O vibration), this result is consistent with that reported previously [33]. For RGO and MG-25, these vibrations become much poor, it is indicated that the large oxygen-containing groups was removed.

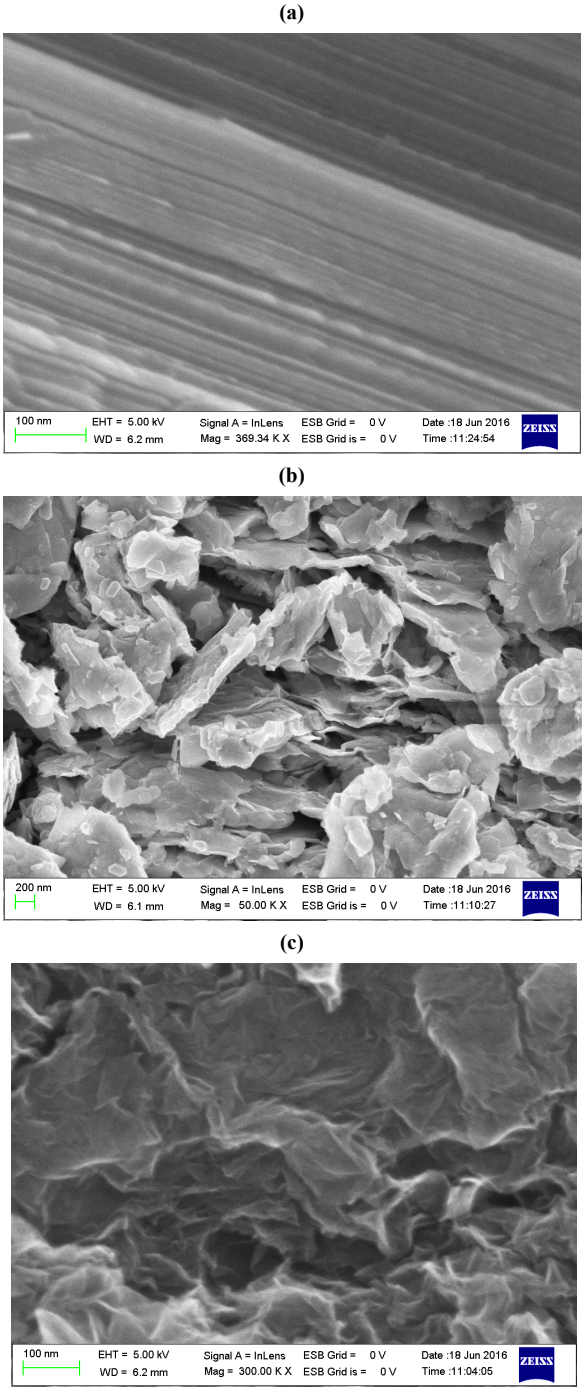

Figure 2.FESEM images of (a) bulk MoS_2, (b) Restack MoS_2, (c) RGO, (e) EDX spectrum of MG-25, (f) HRTEM images of MG-25.

Raman spectroscopy was extensively used to further identify vibrational mode, formation of GO and MG-25. As shown in Figure 4, the two dominant peaks at 1364 and 1599cm^{-1} correspond to D and G bands, respectively,were observed related to GO [27]. In MG-25, Raman peak at 382cm^{-1} and 404cm^{-1} can be ascribed toE^1_{2g} and A^1_g modes of MoS_2 [34], and beside another two peaks around 1341 cm^{-1} and 1580 $cm^{-1}$are the D-band and G-band of RGO have been observed.This result further confirms that RGO has been added into MoS_2 successfully.

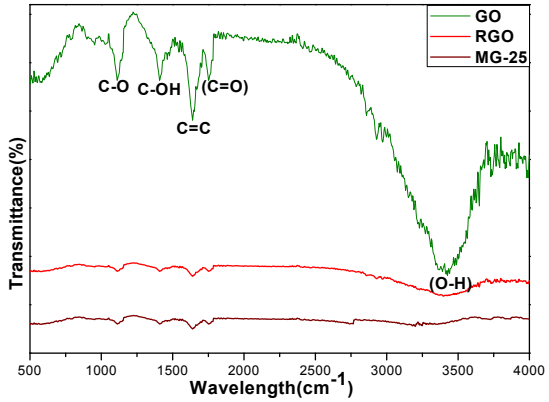

Figure 3 FT-IR spectra of as-prepared GO, RGO and MG-25samples

Photocatalytic measurement

The Photocatalytic activities of Restack MoS_2, MG-12 and MG-25 were performed in RhB aqueous solution under visible light illumination. It is well known that the adsorption of

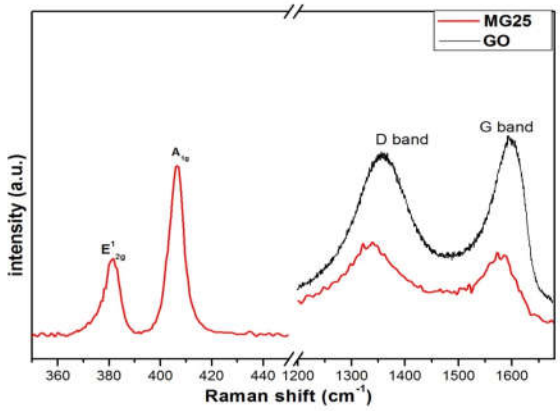

Figure 4 Raman spectra of GO and MG-25 samples.

organic molecules on photocatalyst is an important step during photodegradation process. We firstly investigate RhB adsorption-desorption equilibrium of Restack MoS_2, MG-12, and MG-25 in the dark for 30min. Figure 5 shows the result of RhB adsorption experiments. It is observed that the amount of RGO in the composites is increased with increased absorptivity of RhB molecules, showing that the introduction of RGO improves the adsorptivity of the composites, which is beneficial to photocatalysis process.

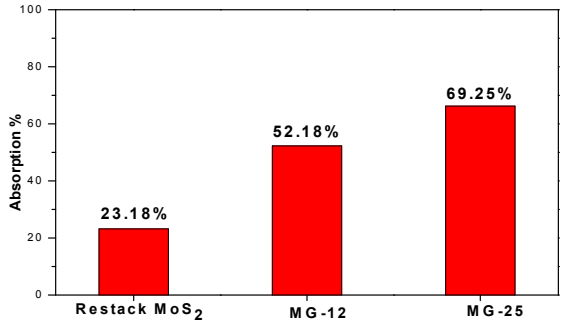

Figure 5. Absorption of RhB after reaching the adsorption equilibrium in the dark.

Generally, the normalized temporal concentration changes (C/C_0) of RhB during the photocatalysis process are proportional to the normalized maximum absorbance (A/A_0), which can be obtained from the change in the RhB absorption profile during the photocatalysis process [35]. Figure 6shows the time-dependent degradation rates of RhB by MoS_2, MG-12, and MG-25 under visible light irradiation. It is observed that, after photocatalytic degradation for 60 min, the concentration of RhB solution decreases by about 27% in the presence of restack MoS_2 synthesized with the same experimental process only without adding RGO. However, the percentage of RGO in the composites increases, as the removal rate is increased to 83% for MG-12 in 60min. In MG-25, it is found that the removal rate can be up to 90% under visible light irradiation for 30min. The result indicating that the photocatalytic performance of MoS_2/RGO composites depends on the proportion of RGO in the composites. The excellent photocatalytic performance should be ascribed tothe enhanced visible light absorption, reduced electron–hole pair recombination, and larger surface area for absorption of dyes.In more detail, firstly, according to the previous data reported in literature on the conduction band, the valence band of MoS_2 and the work function ofgraphene, the energy levels are beneficial to transfer photo-generated electrons from the MoS_2 conduction band to the graphene, which could efficiently separate the photo-generated electrons and holes and improve the light adsorption of MoS_2; secondly, due to a conjugational π-π stacking between the aromatic area of RhB and RGO sheets[36,37].

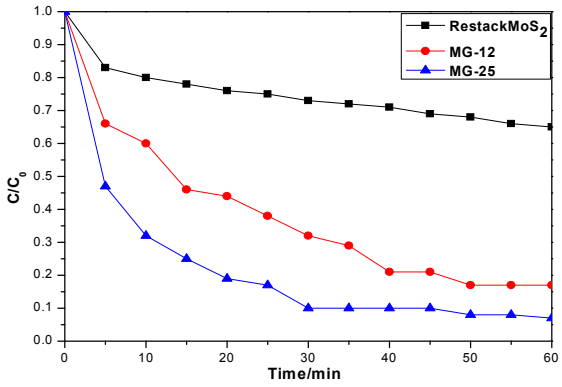

Figure 6 Photodegradation profiles of RhB using various photocatalyst under visible light irradiation.

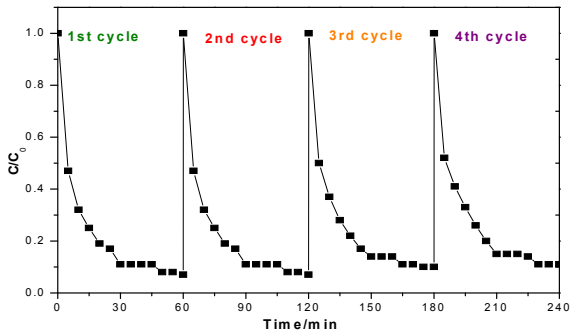

Figure 7 Recycle tests of the MG-25 samples.

Further, the stability of photocatalysts is significant key parameters for its practical applications, the photocatalyst stability of MG-25 was evaluated by checking it's cycling life. In Figure 7, it shows four recycling runs tests on the MG-25 photocatalyst for degradation of RhB under visible light

irradiation. It can be clearly seen that there is only a small loss of photocatalytic efficiency after four successive cycles, which indicates the excellent reusability of catalyst.

The trapping experiments are required to understand the physical mechanism for the excellent photocatalytic degradation properties. Figure 8 presents the trapping experiments of $O_2^{\bullet-}$ radicals and holes results. As well known, methanol and nitrogen are commonly used as the scavenger of $O_2^{\bullet-}$ radicals and holes in photocatalytic degradation reaction, respectively. The photocatalytic degradation efficiency of RhB is 90% without scavengers after irradiation for 30 min, It can be observed that the degradation efficiency decreases from 90% to 55% by 55% if methanol gas is bubbled into RhB solution, but to 69% by 69% if nitrogen is introduced into the solution. It means that both $O_2^{\bullet-}$ radicals and photogenerated holes from MoS_2 are responsible for the photocatalytic degradation activity, but the photogenerated holes dominate the degradation process.

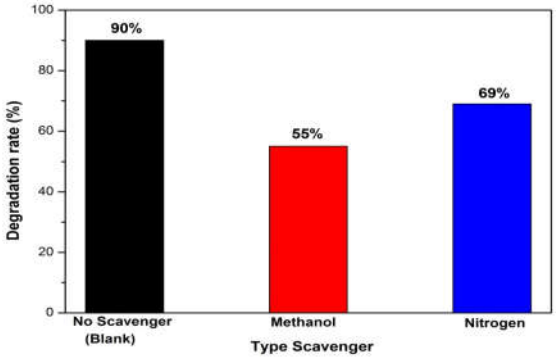

Figure 8 The trapping experiments of $O_2^{\bullet-}$ radicals and holes

Based on these above results, we can conclude that the photocatalytic performances of the MoS_2/RGO composites were better than that of the Restack MoS_2. The physical mechanisms for the photodegradation of RhB over the MoS_2/RGO composites were presented in Figure 9. It's well known that RhB molecules can be excited by visible light and inject electrons and $RhB^{\bullet+}$radicals into the conduction band of MoS_2. Therefore, RhB can be degraded by photosensitization pathway with visible light irradiation.Under the visible-light irradiation also,the electrons are excited to the conduction band (CB) of MoS_2, asthe energy level of RGO is slightly lower than the conduction band of MoS_2 are beneficial to transfer photo-generated electrons from the MoS_2 conduction band to the RGO, and photo-generated holes are left on the MoS_2 at the same time[38, 39] which could result in separation of photo-generated hole-electron pairs on the surface of RGO,which will directly produce reactive oxygen species (ROS) such as $O_2^{\bullet-}$ that could also contribute to degradation of RhB[39]. Moreover, the photogenerated holes on the valence bandof MoS_2 can degrade the RhB molecules adsorbed on the surface of the photocatalysts. Consequently, it suggests that the heterointerface between MoS_2 and RGO could be the main reason for achieving the excellent visible photocatalytic activity in MoS_2/RGO composites.

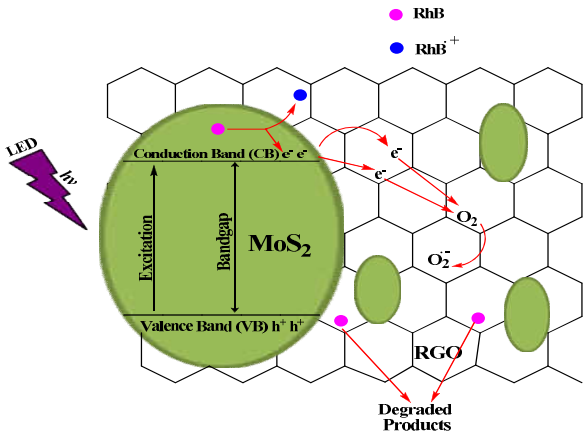

Figure 9 Schematic illustration of the possible mechanism of the photocatalytic activity of MoS_2/RGO composites for degradation of RhB under visible light.

CONCLUSIONS

In summary, the MoS_2/RGO composites were successfully synthesized via a lithiation-assisted exfoliation method and their photocatalytic performances were investigated. HRTEM observation revealed that the MoS_2 nanosheet was densely decorated on the RGO surface. The experimental results indicated that (i) MoS_2/RGO composites exhibit excellent photocatalytic performances under visible light irradiation than Restack MoS_2, and their photocatalytic performances are dependent on the proportion of RGO in the composites; (ii) MoS_2/RGO composite with 0.25 wt% RGO achieves a highest RhB degradation rate of 90% in 30 min. In addition, the cycling tests indicated that the MoS_2/RGO composite have excellent stability, which suggests that the composites are also suitable for optoelectronic devices and sensors applications.

Acknowledgements

The Authors would like to acknowledge the support and help for extending fabrication and characterization facilities, carried out at the Center of Excellence in Nanoelectronics (CEN) under Indian Nanoelectronics Users' Programme at Indian Institute of Technology (IIT), Bombay sponsored by Department of information Technology (DIT) and Government of India. The authors also acknowledge to the management of R.C.Patel Arts, Commerce and Science College, Shirpur for providing the research facilities.

References

1. S. Yang, L. Li, W. Yuan, Z. Xia, 2015 *Dalton Transactions* 44, 6374-6383.
2. E. Kowalska, Z. Wei, B. Karabiyik, A. Herissan, M. Janczarek, M. Endo, A. Markowska-Szczupak, H. Remita, B. Ohtani, 2015 *Catalysis Today* 252, 136-142.
3. Y. Ao, L. Xu, P. Wang, C. Wang, J. Hou, J. Qian, 2015 *Dalton Transactions* 44, 11321-11330.
4. W. Li, Z. Ma, G. Bai, J. Hu, X. Guo, B. Dai, X.2015 *Applied Catalysis B: Environmental* 174, 43-48.
5. W. Zhou, Z. Yin, Y. Du, X. Huang, Z. Zeng, Z. Fan, H. Liu, J. Wang, H. Zhang 2013, *small* 9, 140-147.
6. S. Wi, M. Chen, H. Nam, A. C. Liu, E. Meyhofer, X. Liang,2014 *Applied Physics Letters* 104, 232103.

7. L. A. King, W. Zhao, M. Chhowalla, D. J. Riley, G. Eda, 2013 *Journal of Materials Chemistry A*1, 8935-8941.
8. Y. Li, Y.-L. Li, C. M. Araujo, W. Luo, R. Ahuja, t. 2013 *Catalysis Science & Technology* 3, 2214-2220.
9. M. Remskar, A. Mrzel, M. Virsek, M. Godec, M. Krause, A. Kolitsch, A. Singh, A. Seabaugh, 2011 *Nanoscale Res Lett* 6, 26.
10. S. Min, G. Lu, 2012 *The Journal of Physical Chemistry C*116, 25415-25424.
11. M. A. Lukowski, A. S. Daniel, F. Meng, A. Forticaux, L. Li, S. Jin, 2013 *J. Am. Chem. Soc*135, 10274-10277.
12. F. Meng, J. Li, S. K. Cushing, M. Zhi, N. Wu, 2013 *Journal of the American Chemical Society* 135, 10286-10289.
13. K. Chang, Z. Mei, T. Wang, Q. Kang, S. Ouyang, J. Ye,2014 *ACS nano* 8, 7078-7087.
14. K. S. Novoselov, A. K. Geim, S. V. Morozov, D. Jiang, Y. Zhang, S. V. Dubonos, I. V. Grigorieva, A. A. Firsov, 2004 *science* 306, 666-669.
15. B. Kuchta, L. Firlej, A. Mohammadhosseini, P. Boulet, M. Beckner, J. Romanos, P. Pfeifer, 2012 *Journal of the American Chemical Society* 134, 15130-15137.
16. G.-H. Lee, R. C. Cooper, S. J. An, S. Lee, A. van der Zande, N. Petrone, A. G. Hammerberg, C. Lee, B. Crawford, W. Oliver, 2013 *Science* 340, 1073-1076.
17. V. Chabot, D. Higgins, A. Yu, X. Xiao, Z. Chen, J. Zhang,2014 *Energy & Environmental Science* 7, 1564-1596.
18. Q. Xiang, J. Yu, M. Jaroniec, 2012 *Chemical Society Reviews* 41, 782-796.
19. Z. Chen, S. Liu, M.-Q. Yang, Y.-J. Xu,2013 *ACS applied materials & interfaces* 5, 4309-4319.
20. Y. Chen, H. Ge, L. Wei, Z. Li, R. Yuan, P. Liu, X. Fu, 2013 *Catalysis Science & Technology*3, 1712-1717.
21. N. Zhang, Y. Zhang, X. Pan, X. Fu, S. Liu, Y.-J. Xu, 2011 *The Journal of Physical Chemistry C*115, 23501-23511.
22. L. Pan, X. Liu, Z. Sun, C. Q. Sun,2013 *Journal of Materials Chemistry A*1, 8299-8326.
23. S. Liu, J. Tian, L. Wang, Y. Luo, X. Sun,2012 *Catalysis Science & Technology* 2, 339-344.
24. X. Liu, L. Pan, T. Lv, Z. Sun,2013 *Journal of colloid and interface science* 394, 441-444.
25. Q. Xiang, B. Cheng, J. Yu, Graphene-Based Photocatalysts for Solar-Fuel Generation. 2015 *Angewandte Chemie International Edition* 54, 11350-11366.
26. H. Yoneyama, T. Torimoto, 2000 *Catalysis Today* 58, 133-140.
27. D. C. Marcano, D. V. Kosynkin, J. M. Berlin, A. Sinitskii, Z. Sun, A. Slesarev, L. B. Alemany, W. Lu, J. M. Tour, Improved synthesis of graphene oxide. (2010).
28. S. Stankovich, D. A. Dikin, R. D. Piner, K. A. Kohlhaas, A. Kleinhammes, Y. Jia, Y. Wu, S. T. Nguyen, R. S. Ruoff, 2007 *carbon* 45, 1558-1565.
29. G. Eda, H. Yamaguchi, D. Voiry, T. Fujita, M. Chen, M. Chhowalla, 2011 *Nano letters* 11, 5111-5116.
30. G. Du, Z. Guo, S. Wang, R. Zeng, Z. Chen, H. Liu, 2010 *Chemical Communications* 46, 1106-1108.
31. K. Chang, W. Chen, 2011 *ACS nano*5, 4720-4728.
32. E. Aharon, A. Albo, M. Kalina, G. L. Frey,2006 *Advanced Functional Materials* 16, 980-986.
33. L. Lin, S. Zhang, 2012 *Journal of Materials chemistry* 22, 14385-14393.
34. D. Kong, H. Wang, J. J. Cha, M. Pasta, K. J. Koski, J. Yao, Y. Cui, 2013 *Nano letters* 13, 1341-1347.
35. J. Du, X. Lai, N. Yang, J. Zhai, D. Kisailus, F. Su, D. Wang, L. Jiang, 2010 *ACS nano* 5, 590-596.
36. J. Zhang, Z. Xiong, X. Zhao, 2011 *Journal of Materials Chemistry* 21, 3634-3640
37. X. An, C. Y. Jimmy, Y. Wang, Y. Hu, X. Yu, G. Zhang, 2012 *Journal of Materials Chemistry* 22, 8525-8531.
38. H. Yu, J. Tian, F. Chen, P. Wang, X. Wang,2015 *Scientific reports* 5.
39. L. Zhang, L. Sun, S. Liu, Y. Huang, K. Xu, F. Ma, 2016 *Rsc Advances* 6, 60318-60326.

How to cite this article:

Komal M Sarode *et al* (2018) 'Preparation of Mos2-Graphene Composites with Excellent Photocatalytic Activity Under Visible Light', *International Journal of Current Advanced Research,* 07(1), pp. 9283-9288.
DOI: http://dx.doi.org/10.24327/ijcar.2018.9288.1529

****